High Performance Tokamaks

PJ Knight, CM Roach and DC Robinson
UKAEA Fusion Association, Culham Science Centre, Abingdon, Oxfordshire, OX14 3DB, UK

Introduction

JET has successfully reached its design performance limit, transiently approaching Q~1 in DT operation. For fusion to progress towards a power plant and in particular to assess the effectiveness of alpha particle heating, it is necessary to produce plasmas where alpha particle heating dominates all other power sources. This requires operation in the region Q~10, where $P_\alpha \sim 2(P_{aux}+P_\Omega)$. A number of designs have been proposed to achieve this and related goals (see Table1). In this paper we predict plasma performance in many of these devices by applying the same empirical 1.5-D transport model to all machines, and we then compare the modelled plasma parameters with extrapolations of the usual tokamak operational limits. We have also employed the PROCESS systems code [1] (benchmarked for the ITER-EDA) to produce a self-consistent physics and engineering model and to obtain approximate construction costs.

Machine	*EDA*	*HAM*	*IAM*	*LAM*	*IGNITOR*	*BPX*	*STIGN*
I_p (MA)	21.0	12.7	13.3	17	12.0	10.6	17.0
B_0 (T)	5.68	6.58	5.51	4.23	13.5	8.1	4.0
R_0 (m)	8.14	6.30	6.20	6.45	1.32	2.59	1.32
a (m)	2.8	1.80	1.90	2.33	0.47	0.79	0.94
κ_{95}	1.65	1.61	1.67	1.74	1.85	2.0	2.6
δ	0.24	0.27	0.32	0.34	0.43	0.3	0.2
$q_{a\ 95}$	3.1	3.0	3.0	3.0	3.6	3.3	14.0
q_ψ	3.16	3.03	3.03	2.97	3.12	3.04	10.8
Vol (m^3)	2035	636	720	1166	10.3	62.4	55.6
n_G ($10^{20}m^{-3}$)	0.85	1.25	1.17	1.0	17.28	5.41	6.12
P_{aux} (MW)	100	55	50 (100)	50 (100)	18	20	40
Impurity	2%Be	2%Be	2%Be	2%Be	3%Be	3%Be	3%Be
A_{wall} (m^2)	1665	836	893	1162	50.3	175	126

Table1: Parameters of some proposed high performance tokamaks.

Modelling

The following empirical transport model has been implemented in the ASTRA 1.5-D tokamak transport simulation code [2]. The electron density profile is fixed, and is assumed to be flat with a specified fraction of a single impurity species (Be) and helium ash is included with the density fraction constrained by fixing $\tau_{He}^*/\tau_E=6$. Current diffusion is simulated assuming neoclassical conductivity (with consistent Z_{eff}) and using Hirshman's coefficients for the bootstrap current. The modelled heat sources and sinks include: ohmic and auxiliary power, alpha particle heating, electron-ion exchange, Bremsstrahlung, synchrotron radiation and impurity radiation. Auxiliary power is modelled as a Gaussian deposition profile centred on the magnetic axis of width 0.5a, with equal deposition to electrons and ions. Our empirical model for the thermal diffusivities takes $\chi_i=\chi_e \propto 1/n_e$ and in transport simulations we vary the normalisation constant to assess the sensitivity of plasma performance to the confinement enhancement factor $H_{98PBy(1)}(=\tau_E/\tau_E^{IPB98y(1)})$ over the ITER98PBy(1) scaling law [3]:

$$\tau_E^{IPB98y(1)} = 0.0503 I_p^{0.91} B^{0.08} n_e^{0.44} P^{-0.65} R^{2.05} \kappa_a^{0.72} \varepsilon^{0.57} M^{0.13}$$

Our empirical transport model is weakly sensitive to edge temperature pedestal values which we take as $T_e(a) = T_i(a) =1$ keV in all simulations. In addition we include the Gimblett Hastie sawtooth model to rearrange plasma heat and current inside the q~1 core region when the instability is triggered. For each proposed machine we have performed approximately 20 transport model runs and all reported results are close to being steady-state transport solutions. Calculations with five values of $H_{98PBy(1)}$ were performed at several values of n/n_G.

Results for the Devices in Table 1

Amongst the more interesting results from such calculations are P_{fus}, $Q\sim P_{fus}/P_{aux}$, β_N and

P_{loss}/P_{LH}, where we have extrapolated the anticipated power requirement for transition into H-mode using the recent scaling [3]

$$P_{LH}^{IPB98(5)} = 2.76\bar{n}_{20}^{0.77} B^{0.92} R^{1.3} a^{0.76}$$

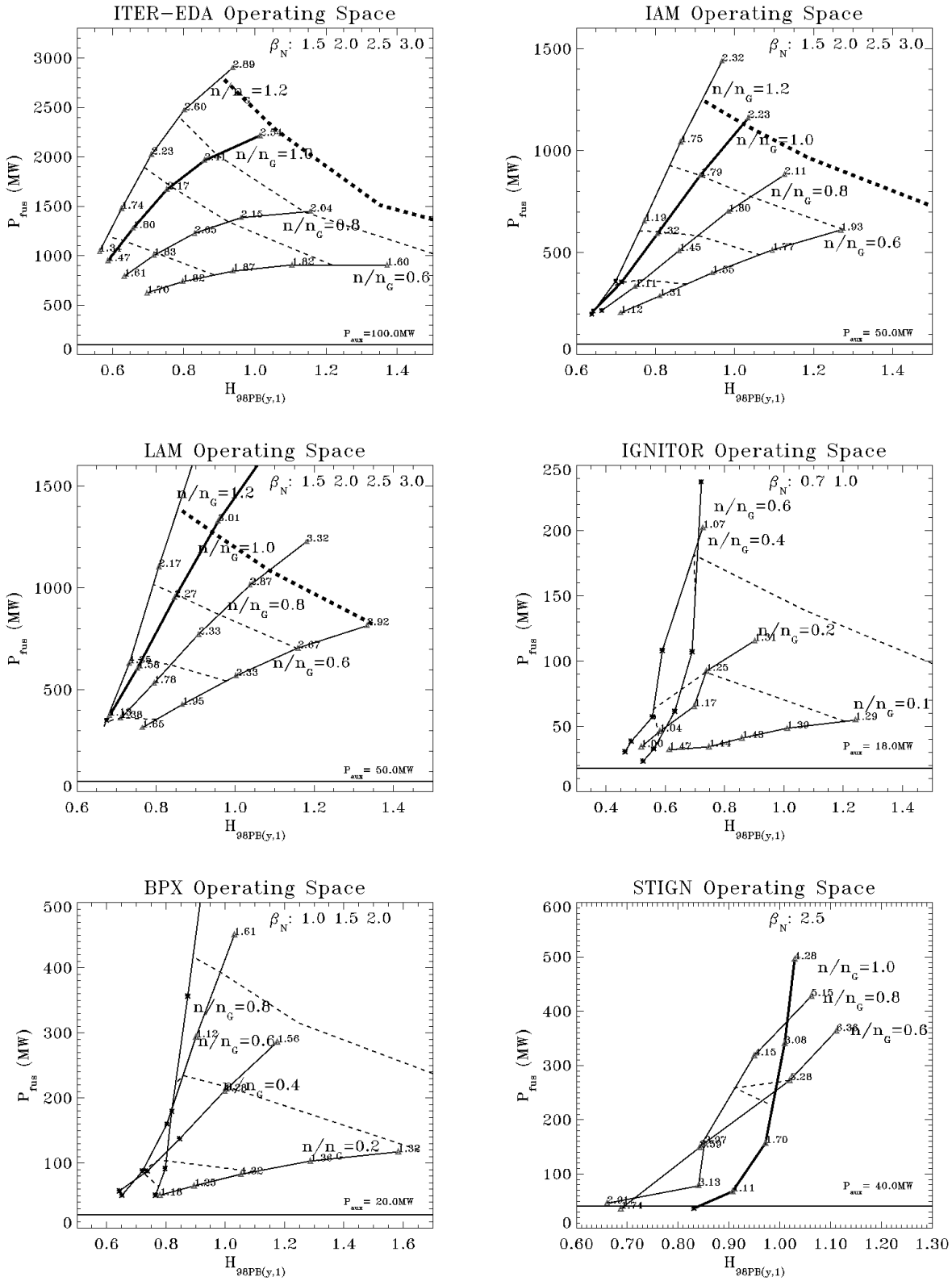

Figure 1: Operating space diagrams for some of the devices of Table1.

Our results are summarised concisely in operating space diagrams, and Figure1 shows these diagrams for each of the proposals in Table1 (except for HAM which is no longer seriousl considered by the ITER JCT owing to marginal P_{loss}/P_{LH}). Each solid curve shows P_{fus} versus $H_{98PBy(1)}$ for a fixed n/n_G. At calculation points where the LH transition threshold power is exceeded P_{loss}/P_{LH} is annotated as a number: otherwise points where P_{loss} lies below the threshold power are instead marked by an asterisk. The dashed curves are interpolated β_N contours**,** and thick solid and dashed curves denote $n/n_G=1$ and the nominal beta limit at $\beta_N=3$ respectively. Finally the auxiliary power P_{aux} is given as a horizontal line.

Figure 1 illustrates our transport model prediction that the ITER-EDA can achieve Q=10 operation with a significantly larger confinement margin than the RC-ITER designs IAM and LAM, and that the LAM machine has a slightly better margin than IAM. Overcoming the extrapolated LH transition power also appears to be slightly more difficult in the IAM machine than in the LAM. The smaller high current and magnetic field machines IGNITOR, BPX and STIGN are proposed as cheaper alternatives to study burning plasmas but, unlike the RC-ITER devices, they are not explicitly intended for high performance steady state operation. IGNITOR and BPX have high magnetic fields and current densities and thus have low beta and high Greenwald density limit. The available auxiliary heating, however, seriously limits the maximum density at which significant P_{fus} can be obtained, and access to H-mode particularly in IGNITOR and BPX requires low density operation giving less P_{fus} and low Q. On the contrary, the STIGN device would be expected to access H-mode without difficulty at high densities and hence attain high Q. While the low aspect ratio tokamak confinement database is sparse, the START experiment has measured values of $H_{98PBy(1)}$ up to ~1.2.

Higher Elongation Devices

Most global confinement scaling laws (eg ITER98PBy(1)) suggest improved confinement at higher I_p and κ. MHD kink modes limit I_p with the constraint $q_\psi^{95} \geq 2$, where

$$q_\psi^{95} = q_* f(\varepsilon) \quad \text{where} \quad q_* = \frac{5a^2 B}{RI}\frac{\left(1+\kappa^2\left(1+2\delta^2-1.2\delta^3\right)\right)}{2} \quad \text{and} \quad f(\varepsilon) = \frac{\left(1.17-0.65\varepsilon\right)}{\left(1-\varepsilon^2\right)^2}$$

At fixed q_ψ^{95} plasmas with higher κ (also higher δ and lower ε) carry significantly higher I_p. Thus higher elongation may improve machine performance both directly from the increased κ, and indirectly through increased capacity for I_p. Taking the transported loss power (neglecting Bremsstrahlung) from $\tau_E^{IPB98y(1)}$ scaling law

$$P_L = \frac{3nTV}{\tau_E} = \left(\frac{3nTV}{0.0503HI_p^{0.91}B^{0.08}n_e^{0.44}R^{2.05}\kappa_a^{0.72}\varepsilon^{0.57}M^{0.13}}\right)^{2.86}$$

and fixing q_ψ^{95} so that $I/aB=5\varepsilon(1+\kappa^2)/(2\,q_\psi^{95})\,f(\varepsilon)$, and with $P_\alpha = 0.25n^2\langle\sigma v\rangle E_\alpha V$, we readily obtain:

$$\left(P_\alpha/P_L\right) \propto \varepsilon^{3.11}\kappa^{3.2}.$$

Thus at fixed q_ψ^{95}, fusion performance is extremely sensitive to κ and ε.

We have applied our transport model to designs with higher κ: various sizes of machines have been modelled (see Table2) to assess whether high performance tokamaks with smaller R can indeed be designed in this way. Figure2 gives operating space diagrams for these devices, some significantly smaller than RC-ITER designs. Our empirical transport model

Machine	*DCR1*	*DCR2*	*DCR3*
I_p (MA)	13.0	13.0	8.8
B_0 (T)	6.2	6.2	6.2
R_0 (m)	5.0	4.3	2.9
a (m)	1.58	1.37	0.95
κ_{95}	1.97	2.0	2.0
δ	0.32	0.32	0.32
q_a	4.2	3.7	4.3
q_ψ^{95}	4.01	3.51	3.73
Vol (m^3)	480	310	101
n_G ($10^{20}m^{-3}$)	1.66	2.2	3.1
P_{aux} (MW)	50 (80)	50 (60)	31
Impurity	2%Be	3%Be	3%Be
A_{wall} (m^2)	675	501	235

Table2: Parameters for higher elongation devices of various sizes.

indeed suggests that promising performance ($Q \gtrsim 10$) may be achieved.

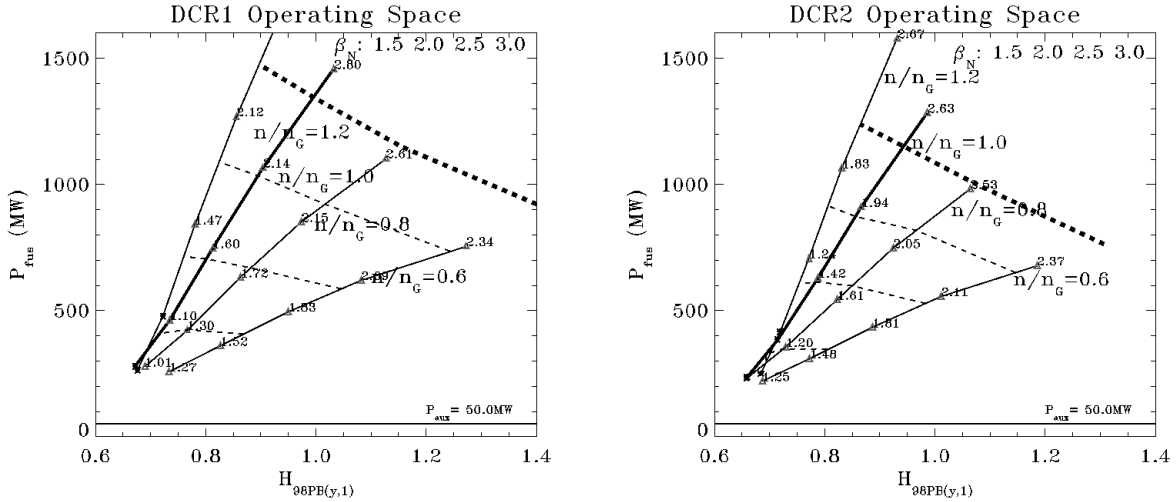

Figure 2: Operating space diagrams for the higher elongation devices of Table 2.

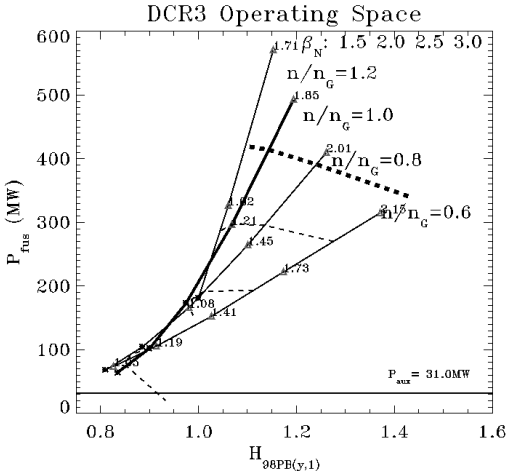

The transport model underpinning these results extrapolates significantly in κ from the existing confinement database. Both the validity of this extrapolation and the engineering issues which are associated with high κ need to be addressed more fully.

Summary

The operating space has been investigated for a number of proposed Next-Step and burning plasma devices, and the same transport model has been applied to all designs to facilitate machine comparisons. Anticipated values of β_N and P_{loss}/P_{LH} have also been calculated, both to assess the proximity of the operating point to the beta limit and the accessibility of H-mode. We also outlined some possible benefits of higher κ and have investigated a range of such devices with various sizes. The favourable dependence of plasma performance on elongation from our empirical model should be verified: a valuable extension of this work is to repeat these calculations, replacing our empirical transport model by physics-based models which have been benchmarked against experimental data. It is also vitally important to assess in detail the impact of engineering issues on the design of the more highly elongated devices.

Acknowledgement

This work was supported by the UK Department of Trade and Industry and Euratom.

References:

[1] UKAEA Fusion Report UKAEA FUS 333: Fusion Economics (Note for the 1996 European Fusion Evaluation Board), TC Hender, PJ Knight, I Cook, May 1996

[2] GV Pereverzev et al, 'An Automatic System for Transport Analysis in a Tokamak', IV Kurchatov Institute of Atomic Energy Preprint, IAE-5358 (1992).

[3] Chapter 2 of ITER Physics Basis, 'Plasma Confinement and Transport', to be published in Nuclear Fusion (1999).